Engineering Journal of Qatar University, Vol. 4, 1991, p. 157 - 177.

STRUCTURAL DESIGN OF ARCH PROFILE AND DEPTH — A COMPUTER-AIDED STUDY

M. H. El-Haddad and G. S. A. Shawki
Faculty of Engineering, Qatar University, Doha, Qatar — Arabian Gulf

ABSTRACT

This paper presents a comparative study of some of the best known and widely used arch profiles, in an endeavour to investigating their structural performance and to determining optimum arch form and depth.

Arch profiles herein studied comprise three categories, namely:

1) Profiles each with one center on axis of symmetry,

2) Profiles with two centres symmetrically disposed on arch base,

3) Profiles with three centres, two of which are located at the extrados points of base while the third common center is positioned on the axis of symmetry.

For all these profiles, both bending moment and normal force distributions are obtained using the stiffness matrix method, the arch being subdivided into twenty elements. Computations were run on computer.

This study shows that while the lancet and segmental arch types rank best among the investigated arch profiles, the horseshoe profile proved to possess the least favourable form in as far as developing stresses are concerned.

NOMENCLATURE

A	Cross sectional area of arch
b	Thickness of arch cross section, Fig. (5)
f_m	Non-dimensional bending moment parameter = M/PL^2
f_n	Non-dimensional normal force parameter = $2\ N/PL$
H	Total height or rise of arch
h	Depth of arch cross section, Fig. (5)
I	Moment of inertia of arch cross section
L	Span length of arch
M	Bending moment resulting from load P
N	Normal force
P	Uniformly applied load per unit of projected length of arch
Q	Shearing force
R	Major radius of arch, Fig. (4)

r	Minor radius of arch, Fig. (4)
S	Half span length, Fig. (2)
V	Height of canopy, Fig. (4)
X	Horizontal distance along base length measured from end of base, Fig. (2)
σ_t	Applied tensile stress
σ_c	Applied compressive stress
σ_{at}	Allowable tensile stress
σ_{ac}	Allowable compressive stress
θ	Angular orientation of major radius of arch, Figs. (4) & (5)

EVOLUTION OF THE ARCH

Man has always strived at finding ways and means of spanning or covering an opening. The use of simple flat beams set a limit to the extent of span that would be covered by such structural element. Man then discovered the so-called arch which can span greater distances and sustain heavier loads than the simple horizonal beam can. After some experience with the false arch, the true arch came into existence.

False Arch

The false, corbelled or cantilevered arch, Fig. (1) [1], as consisting of progressively overhanging or protruding horizontal blocks, slabs or beams was well known to ancient civilizations like China for instance. The prehelenic people of Crete and Greece knew only the corbeled arch.

True Arch

The true arch, however, with its wedge-like ring stones, which constitutes one of the most important and fundamental structural forms appeared, for the first time, in Mesopotamia about 3000 B.C., [2]. It was used in Egypt as early as 2500 B.C.

The earliest form of a true arch was simply a semi-circle, though many variants evolved in the course of time, Fig. (1), [1]. It is not herein intended to make an exhaustive study of all arch variants, but rather to point out briefly to the development of certain forms which are of direct interest to our present investigations. Such forms include semi-circular, segmental, horseshoe and lancet profiles.

Semi-Circular Arch

The semi-circular arch did not become an element of design until about the 8th Century B.C. when the Assyrians used it in building their palaces. It is rather peculiar that the arch was entirely ignored in Greek building construction while

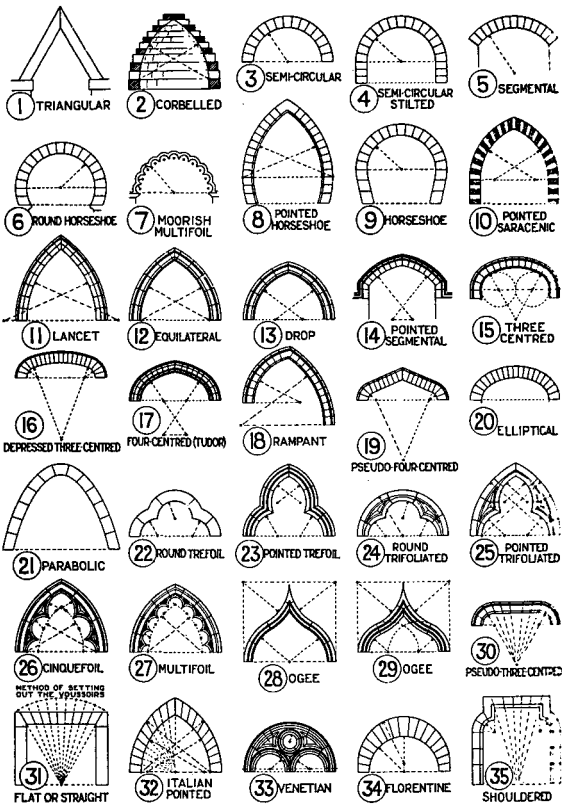

Fig. 1: Various forms of arch people.

Romans used it extensively, e.g. in great aqueducts, bridges and vaults. To mention but few examples are the Aqueducts: Appia, Marcia (carried on stone arches for over ten kilometres), Claudia and Segovia, also bridges such as Pont du Sommieres and Pont du Gard at Nimes in Southern France.

The first three centuries of Roman empire witnessed increased usage of arches hand in hand with the construction of large scale vaults. The expert who could build arches was called, in the Roman Empire (31 B.C. - 5 C.), "Architectus", this being derived from the word "arch" (from Latin arcus = arc and Roman = arca – in Greek: arkhi & arkos mean chief or head).

The first book on architecture was named "De Architectura" and was written by Marcus Vitruvius Pollio who flourished in the period 46-25 B.C.

Arch Profiles other than Semi-Circular

Non semi-circular profiles seem to have been largely appreciated by the Sassanid Persians who used them in their palaces at Ctesiphon near Baghdad. Such profiles are also to be seen in the great arches supporting the domes of Hagia Sofia (537 A.D.) in Constantinople (now Istanbul).

Pointed arches were already known in the 7th century when the Arabs conquered Syria and Persia. By the end of the 8th century, Islamic architecture began to depart radically from Hellenistic and Byzantine Conventions. Arabs were not only responsible for popularising the pointed arch but they have created other forms such as the horseshoe arches, multi-lobed arches and spherical triangle pendentive (stalactite) arches. They have also invented intersecting, joined and lapping arches. These innovations constitute some of the landmarks of Islamic architecture, [3-5].

The renaissance witnessed, however, a strong reaction against the pointed arch in favour of the semi-circular profile which was profusely used in the Roman Empire.

SCOPE OF PRESENT INVESTIGATION

No doubt the vast variation in the form of arch profile, as displayed in Fig. (1), can be attributed mainly to aesthetic considerations. It is herein intended, however, to conduct a comparative study of the structural performance of some of the most commonly used arch profiles, namely:

1. **Single-centred arch,** i.e. arch with its centre lying on the axis of symmetry of the arch, e.g. the semi-circular, the segmental and the horseshoe arches, Fig. (2).

2. **Two-centred arch,** i.e. arch with one centre for each of its two halves, e.g. pointed lancet arches, Fig. (3).

3. **Three-centred arch,** i.e. arch with two halves, each half composed of two circular arcs with their centres lying on one line emanating from the end of the base, the larger radius being equal to the span, e.g. round lancet arches, Fig. (4). (It should be noted that the centres of the two smaller radii, r coincide with each other on the line of symmetry thus confining the number of centres to three.)

For all these profiles, both bending moment (M/PL^2) and normal force ($2N/PL$) diagrams were obtained, Figs. (5) to (11). Moreover, the relevant depth of arch was calculated for three different criteria, Figs. (12) to (15), with a view to determining the optimum depth profile of the arch.

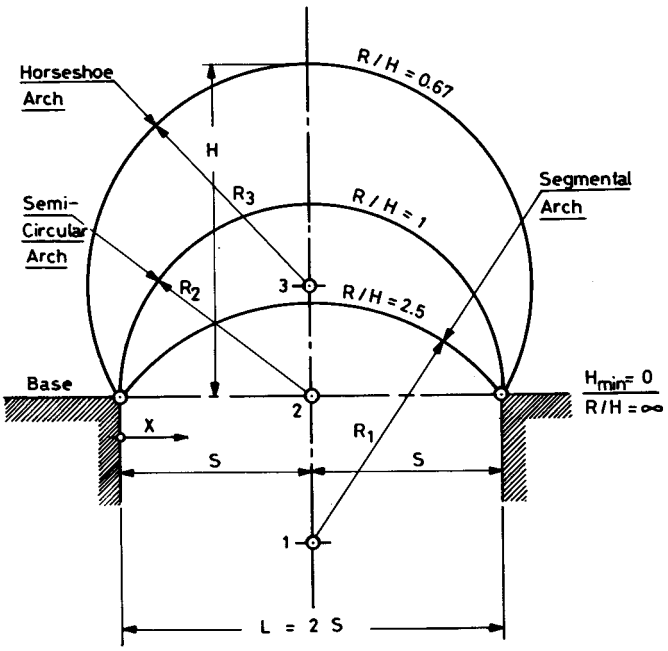

Fig. 2: Arch profiles with centres located on common axis of symmetry. (Category 1).

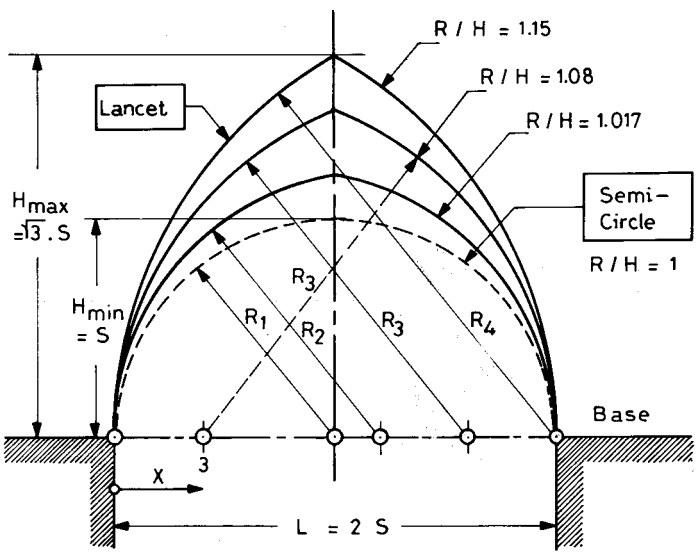

Fig. 3: Arch profiles with two centres located on common base line. (Category 2).

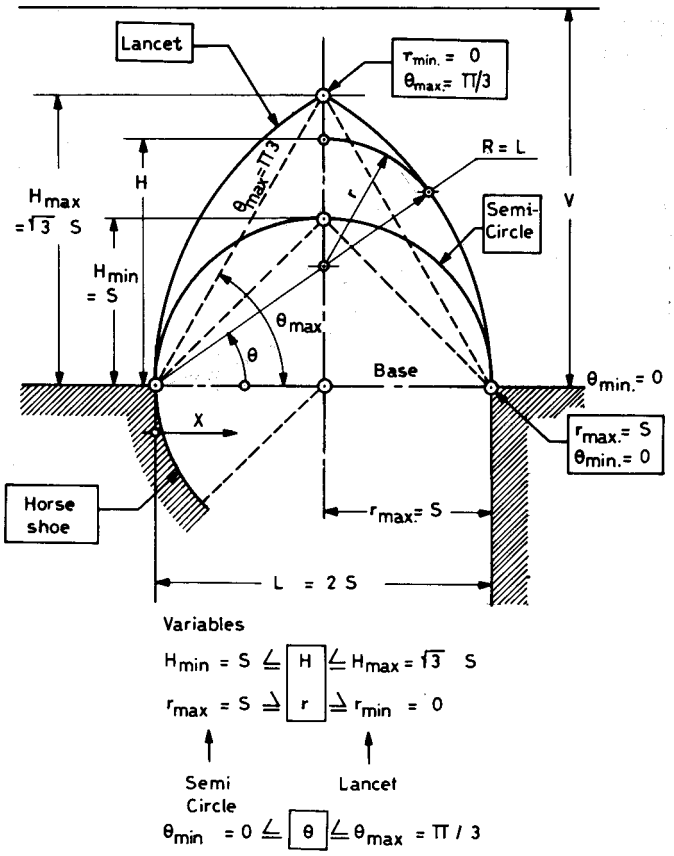

Fig. 4: Arch profiles with two centres one at extrados of base and the other on axis of symmetry. (Category 3).

METHOD OF STRUCTURAL ANALYSIS

Based on the stiffness matrix method, a computer programme [6,7] was used to obtain internal normal force and bending moment distributions for various arch profiles. This programme is based on a linear elastic small displacement analysis using the well known displacement procedure, in which displacements are the unknown quantities. This programme takes into consideration both axial and flexural deformations resulting from axial forces and bending moments respectively.

According to the stiffness matrix method, the arch was idealised as an assemblage of discrete elements interconnected at a finite number of joints called nodes. As the number of joints increases, more accurate results would be obtained.

In the present work arches are divided into twenty-one nodes and twenty elements, Fig. (5). The origin of global axes is assumed at node (1) and the co-ordinates of twenty-one nodes are entered into the input file. The areas and moment of inertia of the twenty elements are assumed constant; they are also entered into the file. Local stiffness matrices for elements are obtained and then used to formulate the overall structural stiffness matrix of the complete arch referred to global axis, Fig. (5). The global stiffness matrix of the complete arch is modified for displacement boundary conditions. In the present study, arches are assumed hinged at both ends, Fig. (5), consequently horizontal and vertical displacements were neglected at these ends. The solution of equilibrium equations results in three displacement components at each joint as rising from the loads applied to the arch. The internal normal force: (N), shear force (Q) and bending moment (M) were calculated for all twenty members of the arch from the displacement and local element stiffness. It should be noted that a vertical uniform load of intensity PkN/m on horizontal projection was applied on all arch profiles studied so as to compare internal forces developing therein.

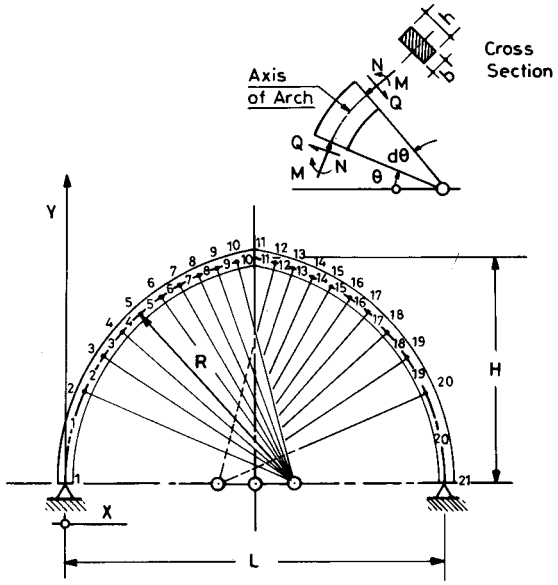

Fig. 5: Computer-aided analysis using the stiffness matrix method.

Fig. (6) displays typical computational results of bending moment and normal force resulting from the live load PkN/m for an arch profile of category (2) with R/H = 1.017. Values of bending moment and normal force are given in the nondimensional forms: M/PL^2 and $2N/PL$ respectively. Moreover, the bending

moment and the normal force distributions are plotted along the centre line of the arch and further projected on the base, Figs. (6-a) & (6-b). This latter representation proves to be quite convenient in comparing the structural performance of the various arch profiles. It is worthy to note that bending moment values are plotted on the tension side of the arch. In other words positive and negative values of bending moments correspond to tensile stresses at the arch top and bottom fibres respectively. Although the bending moment reversed its sign through an inflection point of zero value, the normal force diagram maintains the same sign. This indicates that a compressive normal force still acts along the centre line of the arch though with decreasing values, as the top of the arch is approached.

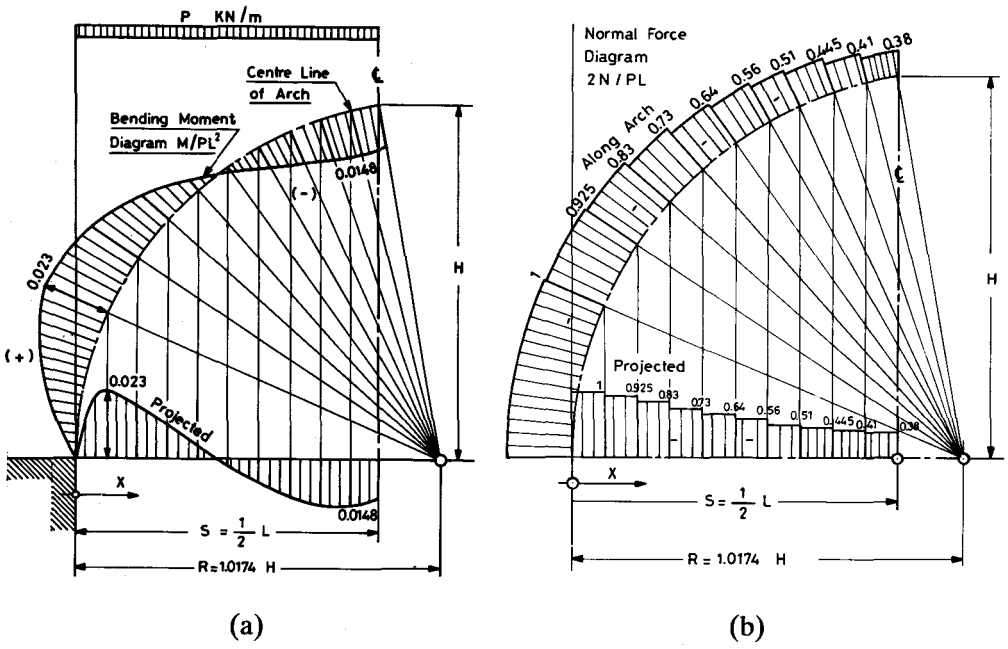

Fig. 6: Typical computational results of bending moment and normal force due to a live load for one of the profiles of Category (2) (R/H = 1.017).

Figs. (7) to (12), also Tables (1) & (2) show the course of variation of bending moment and normal force resulting from the live load P=kN/m for all profiles herein examined. It can be readily seen that for arches of category (1), both bending moment and normal force tend to decrease with increasing values of the ratio X/L, Figs. (7) & (8). The horseshoe arch displays, for the bending moment, appreciably higher values than the rest of profiles, Fig. (7). Values of normal force are shown to decrease with lower values of R/H, Fig. (8).

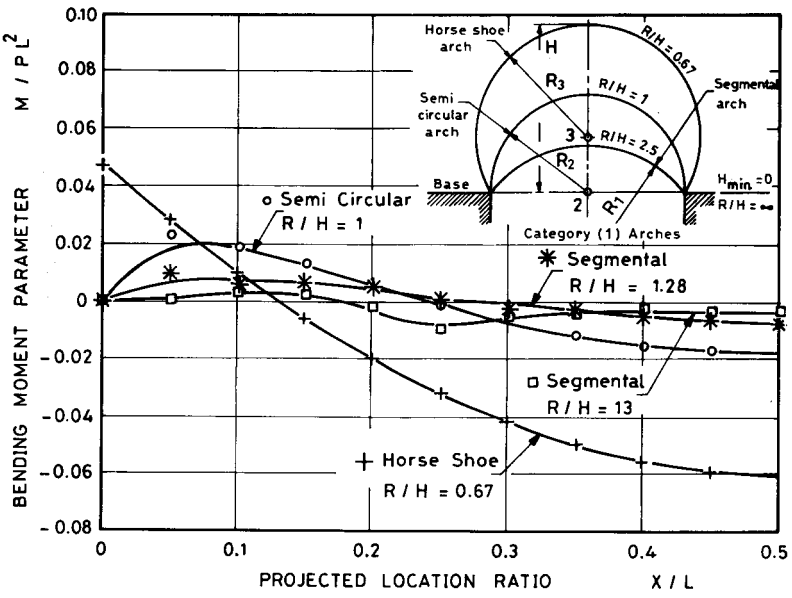

Fig. 7: Comparative results of bending moment for Category (1) profiles.

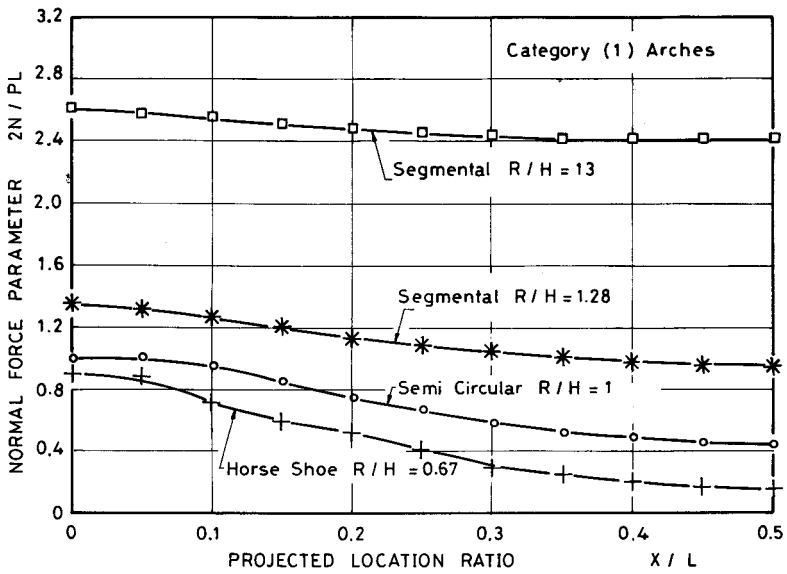

Fig. 8: Comparative results of normal force for Category (1) profiles.

For arches of Category (2), no significant differences in bending moment and normal force values are exhibited by the two-centred profiles, Figs. (9) & (10).

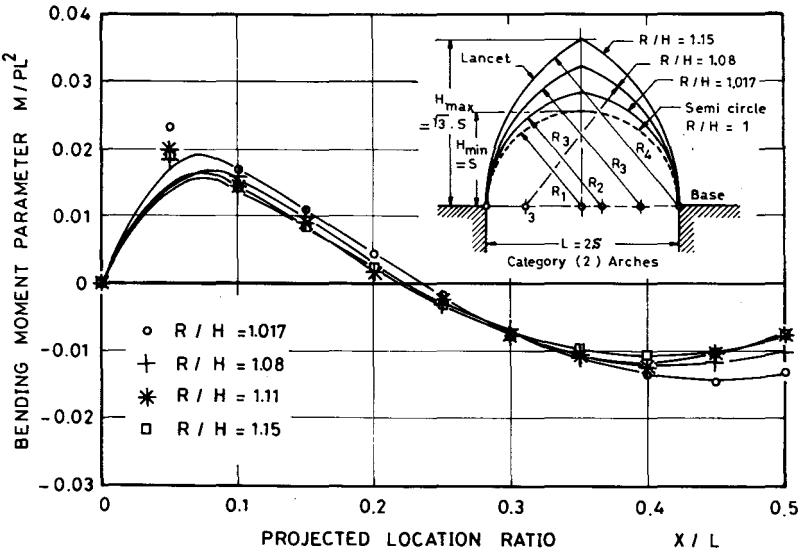

Fig. 9: Comparative results of bending moment for Category (2) profiles.

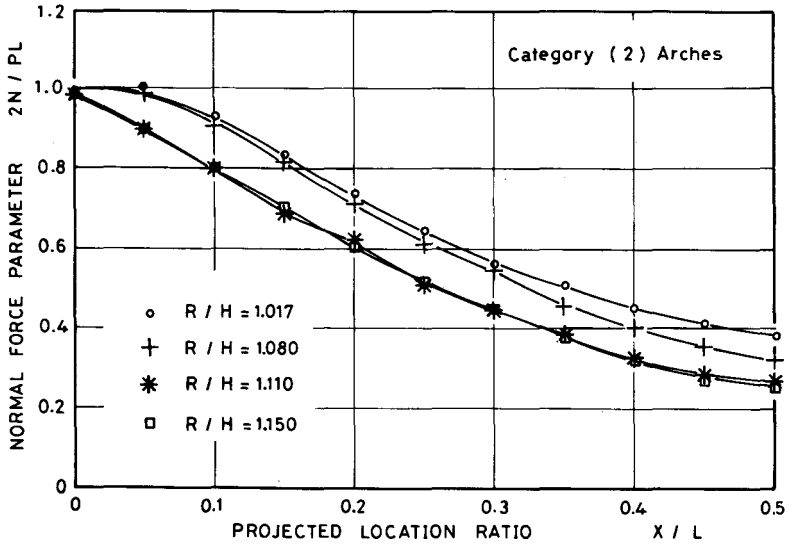

Fig. 10: Comparative results of normal force for Category (2) profiles.

For arches of category (3), the pointed lancet profile (r/R=0) is associated with least bending moment, Fig. (11) and least normal force, Fig. (12), hence it possesses best performance for this category.

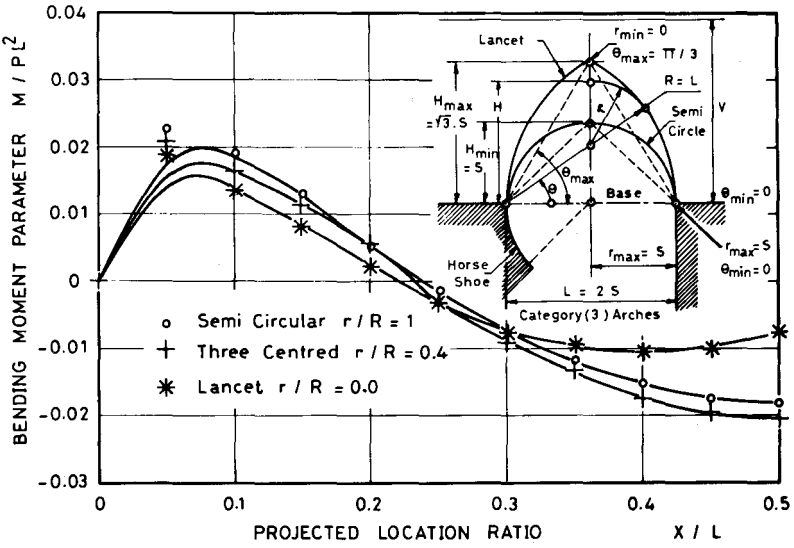

Fig. 11: Comparative results of bending moment for Category (3) profiles.

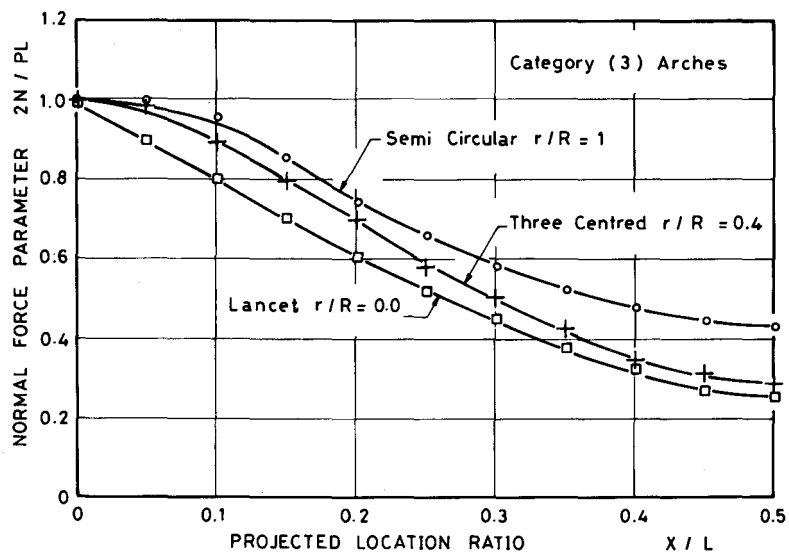

Fig. 12: Comparative results of normal force for Category (3) profiles.

Ranking of profiles would put the pointed lancet and segmental arches at the upper end of the scale and the horseshoe profile at the lower end of the scale, as shown in Fig. (13). As a limiting case, computed results were obtained for R/H = ∞, this being the case, of a straight beam. The maximum value of the non-dimensional bending moment parameter M/PL^2 assumes the theoretical value of 1/8 = 0.125 at mid span.

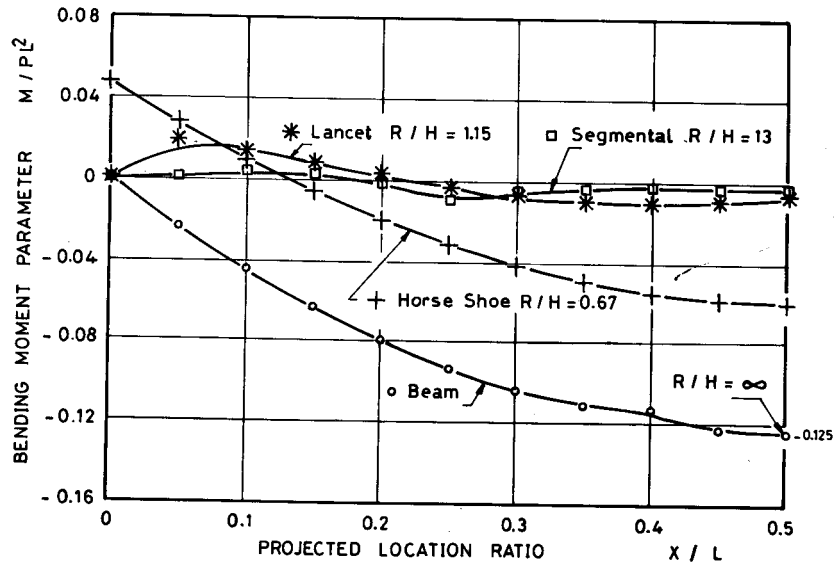

Fig. 13: Comparative results of bending moment for various Categories of arch.

DESIGN CRITERION

Based on the bending moment and normal force values obtained in this study for various arch profiles, normal stresses can be obtained from the theory of elasticity in which the effects of shear deformations are neglected consequently, normal stresses, due to normal force and bending moment can be obtained from the following relationship:

$$\sigma = -\frac{N}{A} \pm \frac{M.Y}{I} \qquad (1)$$

in which A is the cross sectional area of the arch and is equal to b x h, where b and h denote the thickness and depth of the arch respectively.

I is the moment of inertia of the arch cross section; it is equal to $bh^3/12$.

Introducing $f_n = \frac{2N}{PL}$ and $f_m = \frac{M}{PL^2}$, equation (1) would assume the following form:

$$\sigma = f_n \frac{PL}{2bh} \left[(-1 \pm \frac{12L}{h} \frac{f_m}{f_n})\right] \quad (2)$$

Tensile stresses acting on the arch fibres can be calculated from this equation using the positive sign as follows:

$$\sigma_t = f_n \frac{PL}{2bh} \left[-1 + \frac{12L}{h} \frac{f_m}{f_n}\right]$$

Rearranging the terms would assume the form:

$$(\frac{L}{h})^2 - \frac{1}{12} \frac{f_n}{f_m} (\frac{L}{h}) - \frac{2 \sigma_t b}{12 f_m P} = 0 \quad (3)$$

If the material of the arch is not allowed to carry tensile stresses, σ_t in the above equation would be equated to zero; this would therefore lead to the following estimate of arch depth to span ratio (h/L):

$$(\frac{h}{L}) = 12 (\frac{f_m}{f_n}) \quad (4)$$

The above supposition is valid for arch materials weak in tension, e.g. masonry blocks. Based on the above criterion, and with reference to values for f_m and f_n given in Tables (1) & (2) as obtained from the computer analysis programme, estimates of (h/L) can be obtained, Table (3) and Fig. (14) for various types of arch profiles. It can be readily noted that, the depth/span ratio (h/L) corresponding to zero tensile stresses decreases as (R/H) increases. Again the horseshoe profile would require much higher values of depth as compared with other types of arches. This confirms that such profile is not a suitable structural form when compared with other types such as the lancet profile with (R/H) equal to 1.15 or the segmental profile with higher (R/H) values.

The above criterion is considered quite conservative, hence uneconomical from the design point of view as most materials of construction can sustain some tensile stress. In a recent investigation [8] it was shown that the tensile strength of masonry blocks of which most arches are made, attained a value of some 1 MPa. Some tests have indicated, however, that failure can occur by separation between masonry block and mortar materials when tensile stresses reach some 0.20 MPa [8]. This latter value could therefore be used in designing against tensile failure in classical

Table 1
Non-dimensional Bending Moment Parameter: $f_m = M/PL^2$

X/L	Category 1 (One Centred)				Category 2 (Two Centred)				Category 3	Beam
	Semi Circle R/H = 1	Horseshoe R/H = 0.67	SEGMENTAL R/H = 1.28	SEGMENTAL R/H = 13	Drop R/H = 1.017	Drop R/H = 1.08	Drop R/H = 1.11	Lancet R/H = 1.15	Two Radii r/R = 0.4	R = ∞
0.00	0.00	0.0472	0.00	0.00	0.00	0.00	0.00	0.00	0.00	0.00
0.05	0.0277	0.028	0.00914	0.0002	0.023	0.0187	0.0198	0.0188	0.0206	−0.024
0.10	0.0189	0.01	0.0067	0.0029	0.0169	0.0162	0.0145	0.014	0.0165	−0.045
0.15	0.0129	−0.006	0.00672	0.00214	0.011	0.0099	0.99884	0.0082	0.0113	−0.064
0.20	0.0052	−0.0198	0.00457	−0.00213	0.0043	0.0029	0.0013	0.0022	0.0058	−0.08
0.25	0.0016	−0.0318	0.00022	−0.0099	−0.002	−0.0031	−0.00229	−0.0034	−0.0037	−0.094
0.30	−0.0075	−0.042	−0.00164	−0.0056	−0.0078	−0.0067	−0.0073	−0.0079	−0.0092	−0.105
0.35	−0.0122	−0.05	−0.00334	−0.00475	−0.011	−0.0109	−0.0107	−0.0099	−0.0137	−0.114
0.40	−0.0157	−0.056	−0.0049	−0.0026	−0.0137	−0.0126	−0.0126	−0.0108	−0.0178	−0.112
0.45	−0.01784	−0.0599	−0.0068	−0.00535	−0.01475	−0.0118	−0.0105	−0.0105	−0.01998	−0.124
0.50	−0.0186	−0.0613	−0.00754	−0.004	−0.0133	−0.010	−0.0074	−0.0076	−0.0207	−0.125

Table 2
Non-dimensional Normal Force Parameter: $f_n = 2N/PL$

X/L	Category 1 (One Centred)				Category 2 (Two Centred)				Category 3	Beam
	Semi Circle R/H = 1	Horseshoe R/H = 0.67	SEGMENTAL R/H = 1.28	SEGMENTAL R/H = 13	Drop R/H = 1.017	Drop R/H = 1.08	Drop R/H = 1.11	Lancet R/H = 1.15	Two Radii r/R = 0.4	R = ∞
0.00	−1.00	−0.9	−1.35	−2.60	−1.00	−1.00	−1.00	−1.00	0.00	0.00
0.05	−0.99	−0.86	−1.32	−2.57	−0.99	−0.98	−0.98	−0.986	−0.983	0.00
0.10	−0.95	−0.71	−1.265	−2.54	−0.925	−0.913	−0.89	−0.895	−0.895	0.00
0.15	−0.85	−0.59	−1.20	−2.50	−0.83	−0.81	−0.797	−0.796	−0.797	0.00
0.20	−0.74	−0.525	−1.14	−2.48	−0.73	−0.707	−0.685	−0.698	−0.699	0.00
0.25	−0.66	−0.41	−1.077	−2.44	−0.64	−0.607	−0.616	−0.60	−0.528	0.00
0.30	−0.58	−0.30	−1.04	−2.43	−0.56	−0.55	−0.508	−0.516	−0.504	0.00
0.35	−0.52	−0.24	−1.00	−2.407	−0.506	−0.454	−0.445	−0.446	−0.425	0.00
0.40	−0.475	−0.19	−0.97	−2.40	−0.445	−0.40	−0.378	−0.374	−0.346	0.00
0.45	−0.443	−0.16	−0.95	−2.40	−0.406	−0.352	−0.32	−0.316	−0.311	0.00
0.50	−0.43	−0.14	−0.94	−2.40	−0.377	−0.314	−0.275	−0.264	−0.289	0.00

Table 3
Estimated (h/L) ratio for Non-Tensile Stresses

X/L	Category 1 (One Centred)				Category 2 (Two Centred)				Category 3
	Semi Circle R/H = 1	Horseshoe R/H = 0.67	SEGMENTAL R/H = 1.28	R/H = 13	Drop R/H = 1.017	Drop R/H = 1.08	Drop R/H = 1.11	Lancet R/H = 1.15	Two Radii r/R = 0.4
0.00	—	—	—	—	—	—	—	—	—
0.05	0.27	0.644	0.084	0.0009	0.276	0.224	0.24	0.23	0.25
0.10	0.24	0.473	0.064	0.014	0.22	0.213	0.194	0.188	0.22
0.15	0.18	0.20	0.067	0.01	0.159	0.147	0.13	0.124	0.17
0.20	0.084	0.137	0.48	0.01	0.07	0.049	0.023	0.0378	0.10
0.25	0.029	0.58	0.0025	0.049	0.038	0.061	0.045	0.068	0.084
0.30	0.16	1.68	0.0189	0.0277	0.168	0.147	0.172	0.184	0.22
0.35	0.28	2.50	0.04	0.024	0.26	0.288	0.28	0.266	0.39
0.40	0.397	3.50	0.061	0.013	0.37	0.38	0.40	0.35	0.617
0.45	0.48	4.50	0.086	0.02	0.44	0.40	0.39	0.399	0.771
0.50	0.52	5.25	0.96	0.02	0.42	0.38	0.32	0.353	0.86

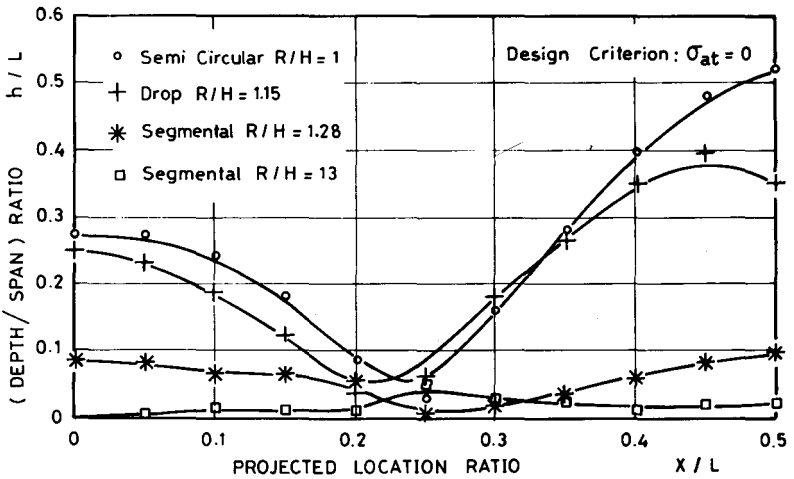

Fig. 14: Calculated arch depth based on the zero tensile stress criterion.

masonry constructions in which mortar serves as bonding material. For other types of constructions, such as arches made of plain concrete, values of allowable tensile stresses can go up as high as 3 MPa depending on the method of construction [9].

Introducing an allowable tensile stress value (σ_{at}) in eqn. (3) the following relationship is obtained:

$$\left(\frac{L}{h}\right)^2 - \frac{1}{12}\,\frac{f_n}{f_m}\left(\frac{L}{h}\right) - \frac{2\,\sigma_{at}\,b}{12\,f_m P} = 0 \qquad (5)$$

the solution of which would lead to:

$$h/L = 1/\left[\frac{1}{24}\,\frac{f_n}{f_m} + \frac{1}{2}\sqrt{\left(\frac{1}{12}\,\frac{f_n}{f_m}\right)^2 + \frac{8}{12 f_m}\left(\frac{\sigma_{at}\,b}{P}\right)}\right] \qquad (6)$$

Based on Eqn. (6), estimates of (h/L) for a semi-circular arch are shown in Table (4) and in Fig. (15) for various values of the non-dimensional parameter (σ_{at} b/P). It can be seen that as the value of this parameter increases, the required depth/span ratio decreases. Even with a value of this parameter as low as 10 the required depth/span ratio would go below some 0.10. For other forms such as the lancet and the segmental profiles, even much lower values of depth/span ratio would be expected.

In addition to designing against tensile failure, arches should also be checked

against compression or crushing failures. This can be achieved by using the negative sign in equation (2), namely:

$$\sigma_c = f_n \frac{PL}{2\,bh} \left[-1 - \frac{12L}{h} \frac{f_m}{f_n} \right] \tag{7}$$

Table 4

Estimated h/L ratio for the Semi-Circular Arch Assumed Allowable Tensile and Compressive Stresses

X/L	σ_{at} b/P				σ_{ac} b/P
	100	**50**	**25**	**10**	**500**
0.00	—	—	—	—	—
0.05	0.0344	0.0474	0.0644	0.0942	0.017
0.10	0.031	0.043	0.0588	0.0855	0.0155
0.15	0.026	0.035	0.048	0.069	0.013
0.20	0.16	0.0215	0.029	0.04	0.0083
0.25	0.0083	0.0065	0.014	0.019	0.0047
0.30	0.0159	0.0273	0.0372	0.054	0.0098
0.35	0.026	0.0357	0.049	0.073	0.0124
0.40	0.0295	0.041	0.057	0.086	0.014
0.45	0.032	0.044	0.061	0.0929	0.0149
0.50	0.0324	0.045	0.063	0.095	0.0195

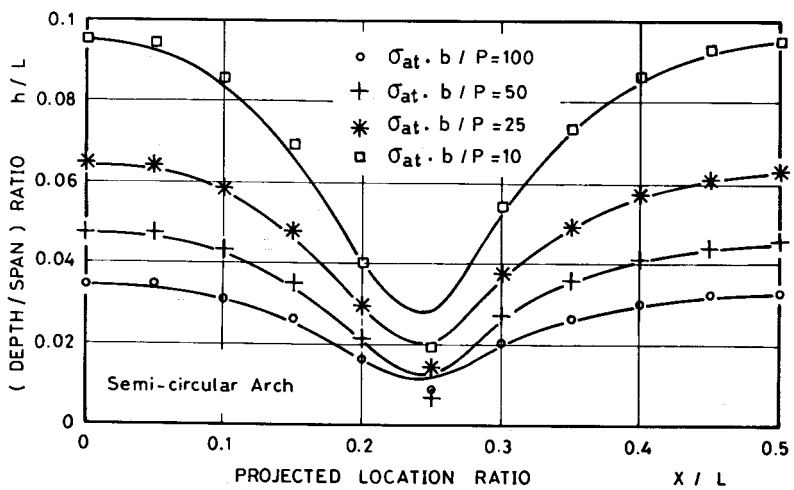

Fig. 15: Calculated depth of semi-circular arch for various values of allowable tensile stress.

Assuming that, σ_c, reaches an allowable compressive strength, σ_{ac}, for arch material, estimates of (h/L) can be readily obtained from the equation:

$$(h/L) = 1/\left[\frac{f_n}{24\, f_m} - \frac{1}{2}\sqrt{\left(\frac{1}{12}\frac{f_n}{f_m}\right)^2 + \frac{8}{12 f_m}\frac{\sigma_{ac}\, b}{P}}\right] \qquad (8)$$

Table (4) & Fig. (16) show estimates of (h/L) as obtained from Eqn. (8) for a circular arch profile calculated on basis of σ_{ac} b/P) = 500. Fig. (16) further displays, for purposes of comparison, (h/L) values for three different design criteria, namely for σ_t = 0 (Eqn. 4), [σ_{at} b/P] = 50 (Eqn. 5) and [σ_{ac} b/P] = 500 (Eqn. 8).

It is worthy to note that the value of (σ_{ac} b/P) is assumed equal to ten times the non-dimensional parameter (σ_{at} b/P) since the compressive strength is at least ten-fold the masonry or concrete tensile strength [9]. Based on this assumption, design against crushing would result in very low values of the depth/span ratio, (h/L) as shown in Fig. (16). This indicates that the first two tensile stress criteria given by equations (4) and (5) should be used; consequently a conservative design would emerge.

Curves displayed in Figs. (14) to (16) are very useful in designing arches; in which a minimum arch depth may well be obtained. For example, the minimum depth for a circular arch profile is shown in Fig. (17) in which the curve corresponding to a value of (σ_{at} b/P) = 50, as per Fig. (15), is used.

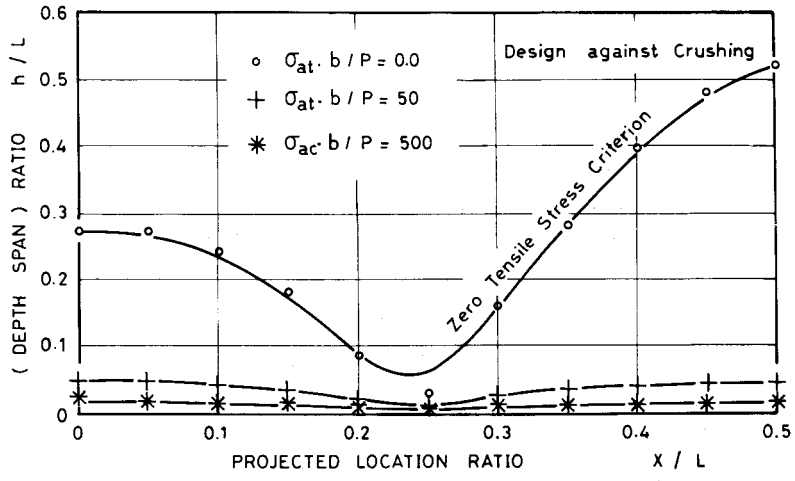

Fig. 16: Calculated semi-circular arch depth for various design criteria.

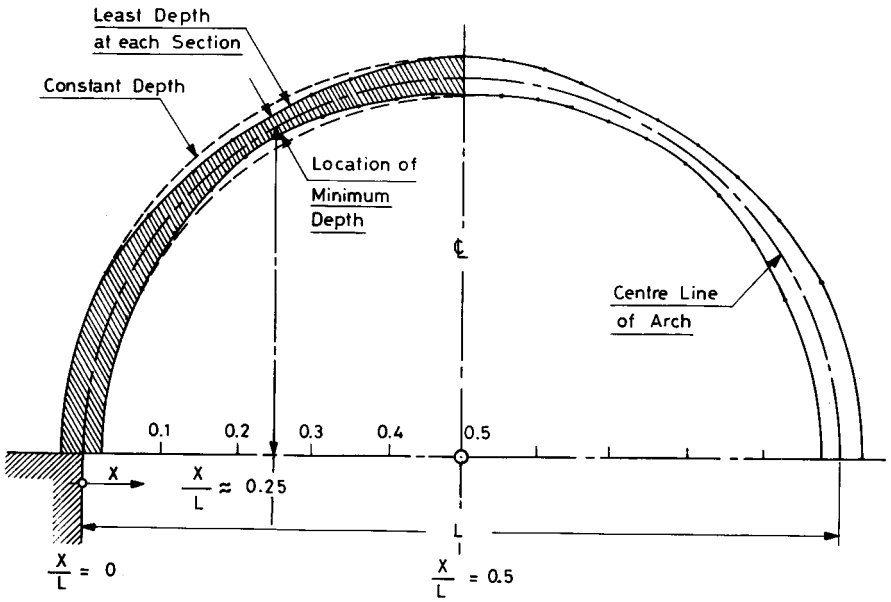

Fig. 17: Minimum circular arch depth for σ_{at} b/P = 50.

SUMMARY & CONCLUSIONS

Based on the stiffness matrix method, a computer-aided analysis is undertaken to obtain both internal normal force and bending moment distributions for the three arch categories investigated.

Computational results while showing marked superiority of lancet and segmental type arches, they exhibit definite inferiority for the horseshoe arch.

Arch depth values, obtained on basis of the zero tensile stress criterion, are shown to be more conservative than those displayed by the crushing stress criterion.

REFERENCES

1. **Sir Bannister Fletcher, 1975,** "History of Architecture", Eighteenth Edition revised by J.C. Palmes, University of London, The Athlone Press, p. 1310.

2. **James Kip Finch, 1960,** "The Story of Engineering", Anchor Books, Doubleday & Company, Inc., Garden City, New York, p. 16.

3. **Cresswell, K.A.C., 1952,** "The Muslim Architecture of Egypt", Oxford.

"A Short Account of Early Muslim Architecture", Harmondsworth and Baltimore, 1958.

"Early Muslim Architecture", Part I, Oxford, 1962.

"Early Muslim Architecture", Part II, Oxford, 1962.

4. **Grube, E., 1969,** "The World of Islam", London.

5. **Derek Hill** and **Lucien Golvin, 1976,** "Islamic Architecture in North Africa", Faber and Faber Limited, London.

6. **El Haddad, M.H., Mahmoud, A.A.,** and **Fahmy, E., 1988,** "Analysis of Thin Walled Cylindrical Shells with Axisymmetric Cracks", Civil Engineering Research Magazine, Faculty of Engineering, Al Azhar University, Vol. 10, No. 1, pp. 77-101.

7. **El Haddad, M.H., El Bahey, M.H.,** and **Samaan, S. 1988,** "Linear Matrix Analysis of Structures Containing Cracks", Res Mechanica, 25 pp. 371-386.

8. **El Nawawy, O.A.,** and **El Haddad, M.H., 1991,** "Prediction of Strength and Fracture Behaviour of Concrete Masonry Wall Units", Proceedings of the Fourth Arab Structural Engineering Conference, Cairo University, Egypt, Vol. IV pp. 195-211.

9. **El Haddad, M.H., El Nawawy, O.A., Fahmy, E.H.,** and **Kandeil, A.Y., 1988,** "Behaviour of Pre-Cracked Plain and Reinforced Concrete Beams", Proceedings of the Third Arab Structural Engineering Conference, Vol. 10, pp. 400-422.